19th Australasian Fluid Mechanics Conference
Melbourne, Australia
8-11 December 2014

Mixing Field Characteristics of Multi-lateral Jets Injected into a Round Pipe Flow

C.X. Thong[1], P.A.M. Kalt[1], B.B. Dally[1], C.H. Birzer[1]

[1]School of Mechanical Engineering
The University of Adelaide, South Australia 5005, Australia

Abstract

Jet in cross-flow is a well-studied and characterised fluid-mixing phenomenon. In several combustion applications, the use of laterally placed side-jets can be used to produce jets into a confined cross-flow (JICCF). These flows can be expected to have similar mixing as the traditional jet in cross-flow cases and therefore provide a potentially cost-effective means of optimising a combusting jet flow. However, there are limits to the data currently available on the fundamentals of JICCF. Hence, the current study investigates the flow structures formed in a round pipe flow modified by four equi-spaced side jets. Non-reacting, isothermal experiments are conducted in water on a central nozzle with four smaller jets located one central diameter upstream of the nozzle exit plane. The induced flow structures are visualised using Planar Laser Induced Fluorescence (PLIF). The operating conditions are varied to explore the role of jet injection to primary flow ratio, whilst the bulk flow rate is maintained at a constant level. The analysed data identify the formation of various flow regimes as the relative momentum-flux ratio induced via side jet injection is increased. The behaviour of the side jets within the main jet is substantially different from similar side-jet injection into an unconfined flow. The results show that several flow regimes can be discerned, namely: a non-impinging flow; impinging flow with no backflow; and impinging flow with backflow. It is found that the mixing trends and resulting regimes have consequences for the emerging near-field mixedness.

Introduction

Combustion is a widely used method to convert the chemical energy that lies dormant within fuels into other forms of energy such as heat, light and kinetic energy. Fuel mixing in combustion is important as combustion can only be achieved when both fuel and air are mixed at the molecular level. To enhance mixing for turbulent jet flames, the method of jets in a confined cross-flow is investigated.

Jets in a confined cross-flow (JICCF) have been studied primarily for the applications in jet-fume dilution and Rich Burn/Quick Quench/Lean Burn (RQL) combustors [5]. The similarity between these applications includes the need for a rapid quenching process, that is, either to reduce a high temperature fume to an acceptable temperature level that is less damaging for turbine materials, or quick quenching from a rich combustion to a lean combustion zone to reduce oxides of nitrogen (NOx) emission [11]. These processes are generally conducted by injecting fluid (air/water) at relatively lower temperature into the rich fume/combustion-product region. The question of applying similar concepts for active turbulent jet flame mixing control and possibility of stabilizing the flame has been raised in light of increased interest in reducing combustion pollutant emission and enhancing flame stability under a wide range of operating conditions.

In many JICCF applications, mixing is reliant on the induced shear vortices, in particularly the Counter-rotating Vortex Pairs (CVP). The CVP phenomenon has been investigated extensively in the Jet in Cross–flow (unconfined flow) studies [9,12]. It is insufficient to rely only on the induced CVPs for turbulent mixing as they do not contribute much to the large scale turbulent structures in the flow, but this can be overcome by impinging the jets upon the confinement wall or on opposing jets [4]. However, most studies on JICCF found that jets impingement may not be favourable for the mixing applications mentioned earlier [3]. This prompted many studies to not probe further into the impinging cases thus contributing to the paucity of data available in this flow mode.

No "rule of thumb" law for good mixing has been established through JICCF studies [5]. The jet penetration into the cross-flow is an important parameter, and on a case by case basis depending on the confinement geometry, it can be characterised by means of the relative jet injection to primary flow momentum-flux ratio, as shown in the equation

$$J = \frac{(\rho V^2)_{inj}}{(\rho V^2)_p} \quad (1)$$

Where J is the momentum-flux ratio, ρ is the respective fluid densities, and V is the respective fluid velocity [5,11].

Most studies conducted on JICCF involve injecting streams of flow into a cross–flow of varying temperature, thus very little information is available on isothermal flow cases. Most studies involve injecting cooler air into air streams of relatively higher temperature, thus profiling the temperature variances at a certain point downstream to quantify for flow mixing [10,11]. The mixing mechanisms are influenced by the fluid density gradient, and thermal and molecular diffusion is not unity for all flows. Through viscosity, temperature also plays a part in mixing intensity [2]. While temperature measurements were conducted at the exit plane and for selective cases, no quantitative data are available on the impact of side injection on the mixing fields inside and outside the primary jet flow.

The current study explores the flow field and development of multiple jets impingement with increasing relative momentum-flux ratio, inside a round pipe in an isothermal flow environment. The aim of the current work is to assess the progression of the flow modes and their corresponding flow structures. This is achieved through an experimental investigation.

Methodology

Experiments were conducted in a water tunnel with a working section measuring 500 × 500 × 1800 mm^3. The experimental arrangement is shown in figure 1. A Perspex pipe with 56mm primary internal diameter (D) is fitted with four radially aligned equi-spaced 6mm Perspex jets located at one primary diameter upstream of the pipe (primary) exit. Perspex pipes are used for

the nozzle construction to allow optical access into the pipe. The region of interest in the nozzle is aligned with the centre of the tunnel's working section.

Flow for both the primary nozzle and side-injectors are sourced from different reservoirs respectively. Primary reservoir is seeded with Rhodamine 6G of concentration 0.1g/400L while the jet–injectors' reservoir comprises of clean water.

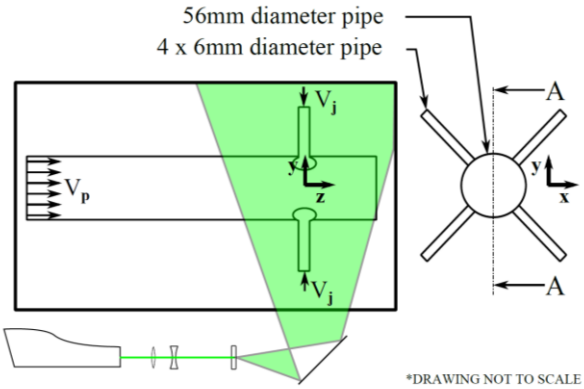

Figure 1. Schematic diagram of the experimental arrangement.

Planar Laser Induced Fluorescence (PLIF) is conducted using a Quantel Brilliant B Nd:YAG twin laser, frequency doubled to 532nm and double-pulsed at 10Hz. An optics train consisting of a combination of cylindrical and spherical optics lenses are used to produce a 2mm thickness laser sheet to illuminate the region of interest.

Images are captured on a Princeton Megaplus II Charged Coupled Devices (CCD) camera with a 2048 × 2048 pixels array. Image collection is done through the software EPIX XCAP 3.8. The camera is fitted with Tamron f1/4D telephoto lens and an addition of orange glass filter to capture PLIF images. The physical imaged spaced is approximated to be 200 × 200 mm^2. The spatial resolution ranges from 10.3 to 10.6 px/mm depending on camera readjustments. The timing for the laser beam discharge and CCD shuttle control is done using a Berkeley Nucleonics Corp (BNC) 565 delay generator.

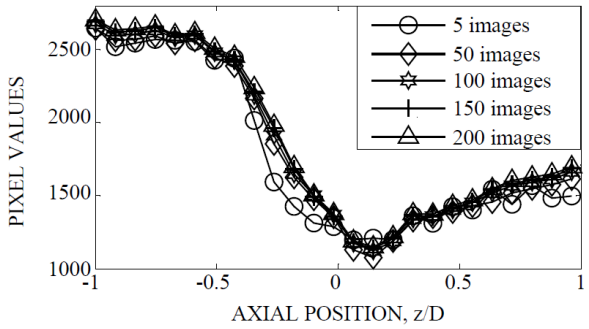

Figure 2. Mean flow centreline pixel values for different numbers of averaged images.

Figure 2 shows the statistics independence test carried out on different number of images in the ensemble of the J = 132 case. As the numbers of averaged images increases from 5 through 200 images, the mean centreline pixel values start converging on a single profile. The profile for 200 images overlaps with that of 150 images. This goes to show that the ensemble of 213 images is sufficient to present the current results.

The ensemble of 213 PLIF images is processed using OMA–X [7] following [6] and [8]. The PLIF images are predominantly calibrated with the unmixed dye solution (100% dye mixture concentration). Each PLIF image is calibrated with the upstream primary flow which remains unmixed with the injections stream.

Momentum-flux ratio, J	**18**	**35**	**58**	**90**	**132**	**186**
Primary Flow rate, $\dot{m}_p$ [L/h]	440.1	425.5	410.8	396.1	381.5	366.8
Injection Flow Rate, $\dot{m}_{inj}$ [L/h]	43.1	57.52	71.9	86.3	100.7	115.0
Massflow ratio, $\dot{m}_{inj}/\dot{m}_p$	0.098	0.135	0.175	0.218	0.264	0.313

Table 1. Experimental flow parameters.

The experimental matrix for the current study is as presented in table 1. The primary flow rate is reduced gradually through the datasets and correspondingly, the injection flow rate is increased to compensate for the loss of primary flow whilst maintaining a constant total flow rate.

Results and Discussion

The x, y and z-axis in the following figures denote the direction into the page, upwards, and stream-wise, respectively. The axial stream-wise distance is normalized to the primary nozzle diameter (D) and z/D = 0 indicates the jet-injectors' location whilst z/D = 1 indicates the nozzle exit.

The typical instantaneous PLIF images in figure 3 show the flow condition for increasing jet-to-primary flow momentum-flux ratio. The large scale mixing structures induced in the flow can be observed qualitatively from the figure. The dye-mixture fraction is obtained by normalizing the local signal values with the unmixed dye signal far upstream of the mixing region. Thus, the dye-mixture fraction value of 1.0 (the brightest region) corresponds to unmixed dye-mixture (purely primary flow fluid) whilst dye mixture fraction of value 0.0 signifies pure jet injection fluid. The increase in relative momentum-flux ratio (J) in figure 3 corresponds to a gradual change in the flow modes.

The streaming flow mode, where separate individual streams are formed, can be seen from figure 3(a). The increase in J leads to jets over-penetration and impinges at a location downstream of the jet–injectors' location in figure 3(b). A further increment in the J (figure 3(c)) shows the jet injections impinging at a shorter distance downstream in comparison to that in figure 3(b). The formation of backflow in the cases with relatively higher J cases can be observed in figures 3(d) through 3(f).

The mean PLIF dye mixture fraction images corresponding to cases shown in figure 3 is compiled from the ensemble average and is presented in figure 4. The different trends corresponding to the increase in J can be better observed through the dye mixture fraction images.

Figure 4(a) shows that little signal is captured of the jet-injection stream (darker region). The J value in this case is relatively lower than the other cases that the injection fluids are convected downstream without much penetration into the flow. The "residual" signal captured in this figure suggests that the flow mixing is reliant on the formation and development of the Counter–rotating Vortex Pairs (CVP).

A triangular jet-injection fluid region can be observed in figure 4(b) and (c). This is akin to a potential core of a simple jet and indicates the impinging of the lateral jets. A transition from impinging to a backflow mode can be observed in figure 4(d). This is characterized by the gradual changes to the downstream

injection fluid profile, that is, the transition from a triangular profile to a thicker stream-like profile.

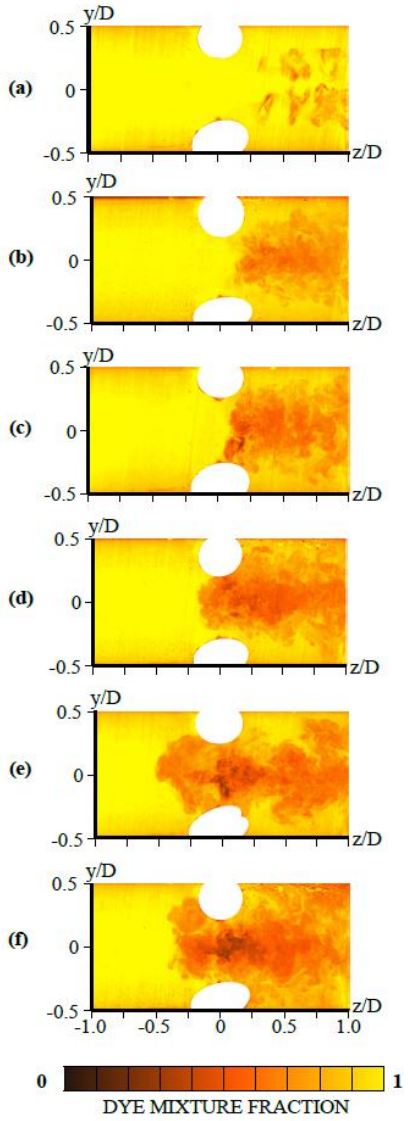

Figure 3. Typical instantaneous image for test cases (a) J = 18, (b) J = 35, (c) J=58, (d) J = 90, (e) J = 132, and (f) J = 186.

Figure 5 shows the centreline dye-mixture fraction profile for all of the investigated cases as indicated by the legends. Observing the profile for case *J* = 18 shows a gradual decrease in dye mixture fraction from approximately z/D = 0.25 onwards. This gradual depreciation from an unmixed dye-mixture plateau of 1.0 is consistent with the gradual penetration of CVPs into the imaged region. Cases from *J* = 18 to *J* = 186 feature a similar plateau region upstream, which corresponds to the unmixed dye region. The axial location when the dye-mixture fraction value begins to decrease shifts upstream with the increase in *J*. Cases with the impinging flow mode, *J* = 35 and *J* = 58 show a sharp drop from the unmixed plateau. Cases with backflow, *J* = 132 and *J* = 186, shows a consistent arch-like profile which is initiated upstream of z/D = 0 as a result of the induced backflow. From the plotted profiles, it is clear that the separate trends can be discerned into separate regimes. A streaming flow mode (such as that in figures 3(a) and 4(a)) is represented by *J* = 18; impinging flow mode is represented by groups of *J* = 35 and *J* = 58; and backflow mode represented by groups of *J* = 132 and *J* = 186.

The mixedness of a flow is an indication to how well the flow mixes in comparison to a homogenously mixed flow. The local mixedness, θ_i for the current study is defined by:

$$\theta_i = \begin{cases} \frac{|(f_i - f_{max})|}{(f_{max} - f_{hom})}, & f_i \geq f_{hom} \\ \frac{f_i}{f_{hom}}, & f_i < f_{hom} \end{cases} \quad (2)$$

Where f_i is the local dye mixture fraction at a local axial location, f_{max} defines the local maximum dye mixture fraction at the unmixed section of the flow, and f_{hom}, the homogenous dye mixture fraction value, defined by

$$f_{hom} = \frac{\dot{m}_p}{\dot{m}_p + \dot{m}_{inj}} \quad (3)$$

Where $\dot{m}_p$ defines the primary flow rate whilst $\dot{m}_{inj}$ defines the injectors flow rate. Mixedness of 1.0 indicates a homogenous mixture whilst mixedness of 0.0 indicates an unmixed flow.

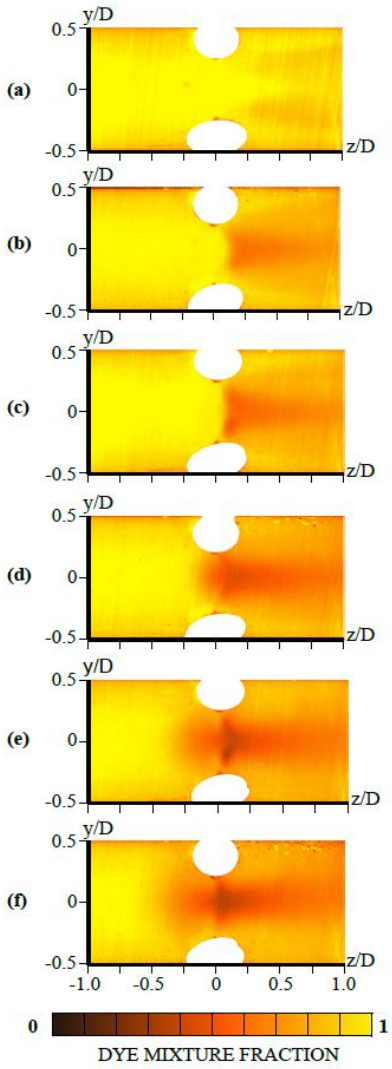

Figure 4. Mean dye mixture fraction images at the centre plane for cases (a) J = 18, (b) J = 35, (c) J=58, (d) J = 90, (e) J = 132, and (f) J = 186.

Figure 6 shows the profile of centreline mixedness for the cases investigated. Differences in mixing trends between case *J* = 18; *J* = 35, 58; and *J* = 132, 186 are noticeable. For *J* = 18, the flow remain unmixed until z/D = 0.25 where it starts to increase to a homogenous mixedness at z/D = 0.8. Despite the homogenous mixing, flames in such mode exits the nozzle in separate individual streams [1].

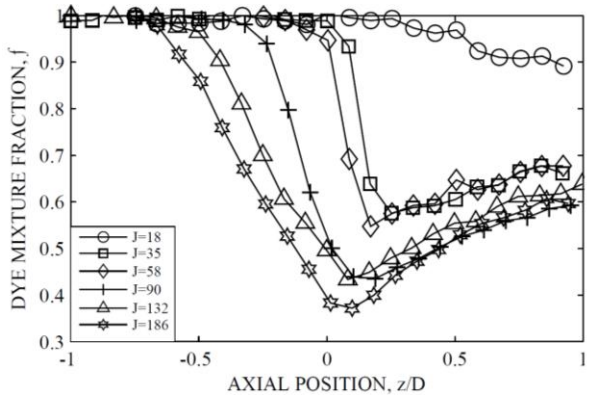

Figure 5. Centreline dye mixture fraction for increasing momentum-flux ratio $18 \leq J \leq 186$.

Similar trends can be observed for cases $J = 35$ and $J = 58$ where the mixedness increases from z/D = 0 and peaks at 1.0 close to z/D = 0.05 before decreasing and increases gradually to 0.8 at the nozzle exit. The spike region correlates well with the jet injections' impingement and over-penetration as discussed before. For cases of $J = 132$ and $J = 186$, the mixedness increases upstream of the jet injectors' location at z/D = 0 by the backflow. A steep increase in mixedness is followed by a recess to a local minimum which anchors onto the jet injections' impingement point. It can also be observed that the mixedness values for $J = 35$, $J = 58$, $J = 132$ and $J = 186$ collapses onto each other at locations $0.5 < z/D < 1.0$. A slight deviation in trend however can be detected for case $J = 90$ which has been identified as the transitioning point from an impingement flow mode to backflow mode.

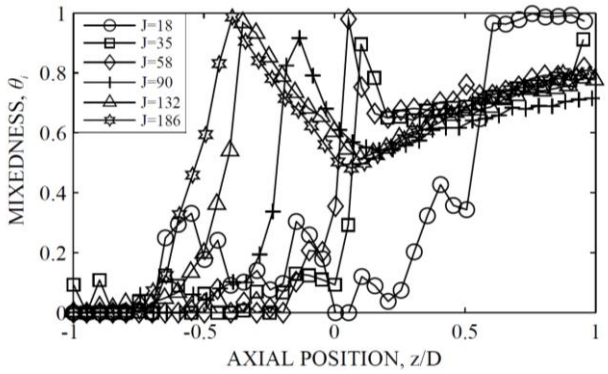

Figure 6. Centreline mixedness for increasing momentum-flux ratio, $18 \leq J \leq 186$.

Most of the other cases ($J = 35$ through 186) show a similar mixedness trend with the exception of case $J = 90$. The characteristic differences between the cases are the initiation point for the dye-mixture fraction in figure 5, which moves progressively upstream with increase J. Correspondingly, the point when the peaks in the mixedness plot also progresses upstream.

The highest mixedness achieved in the current study at the pipe outlet, z/D = 1, stems from case $J = 18$. However, a well-mixed centreline at the outlet should not be taken as a "good" mixing system and due considerations must also be given to the flow exit profiles highlighted in [1]. By comparing the instantaneous and the mean dye mixture fraction image in figures 3(a) and 4(a), it is intuitive to expect separate injection streams to emanate from the nozzle exit into the environment. The "potential core" seen in cases $J = 35$ through $J = 186$ may have a positive influence on the flame stability relative to the flow mode in case $J = 18$.

Conclusions

The current study investigates planar dye-mixture fraction profile in a pipe flow modified by four equally spaced side-jets with water as the working fluid. The primary mass-flow is decreased gradually whilst the injection-flow is increased to keep the total mass-flow in the pipe constant. The scalar field is visualized using PLIF technique.

The instantaneous results of the investigated cases serve as a good initial indication of the mixing intensity inside the pipe. It can be observed that the mixing intensity between the different streams (primary and injection streams) increases with respect to the relative momentum-flux ratio, J. Mean dye mixture fraction images presented show averaged dye distribution for the respective cases from a streaming flow mode to the backflow mode. By studying the centreline flow data, several flow trends can be discerned from the grouping of the centreline flow plots which corresponds to the flow mode: streaming mode; impingement mode; and backflow mode. The transition region from the impingement to the backflow mode is also captured in case $J = 90$.

References

[1] Birzer, C.H., Kelso, R.M. & Dally, B.B., Flame Structure of Jets in Confined Cross-flows, in *Proceedings of the Australian Combustion Symposium*, 2011.

[2] Brown, G.L. & Roshko, A., On Density Effects and Large Structure in Turbulent Mixing Layers, *Journal of Fluid Mechanics*, **64**, 1974, 775-816.

[3] Doerr, T., Blomeyer, M. & Hennecke, D.K., Optimization of Multiple Jets Mixing with a Confined Flow, *Journal of Engineering for Gas Turbines and Power*, **119**, 1997, 315-321.

[4] Gosman, A.D. & Simitovic, R., An Experimental Study of Confined Jet Mixing, *Chemical Engineering Science*, **41**, 1986, 1853-1871.

[5] Holdeman, J.D., Liscinsky, D.S., Oechsle, V.L., Samuelsen, G.S. & Smith, C.E., Mixing of Multiple Jets with a Confined Subsonic Crossflow: Part I-Cylindrical Duct, *Journal of Engineering for Gas Turbines and Power*, **119**, 1997, 852-862.

[6] Kalt, P.A.M., Birzer, C.H. & Nathan, G.J., Corrections to Facilitate Planar Imaging of Particle Concentration of Particle-laden Flows using Mie Scattering, Part 1: Collimated Laser Sheets, *Applied Optics*, 2007, **46**, 5823-5834.

[7] Kalt, P.A.M. & Long, M., OMA for MAC OS X, www.oma-x.org, 2014.

[8] Kalt, P.A.M. & Nathan, G.J., Corrections to Facilitate Planar Imaging of Particle Concentration in Particle-laden Flows using Mie Scattering. Part 2: Diverging Laser Sheets, *Applied Optics*, **46**, 2007, 7227-7236.

[9] Kelso, R.M., Lim, T.T. & Perry, A.E., An Experimental Study of Round Jets in Cross-flow, *Journal of Fluid Mechanics*, **306**, 1996, 111-144.

[10] Kroll, J.T., Sowa, W.A. & Samuelsen, G.S., Optimization of Orifice Geometry for Crossflow Mixing in a Cylindrical Duct, *Journal of Propulsion and Power*, **16**, 2000, 929-938.

[11] Leong, M.Y. & Samuelsen, G.S., Mixing of Jet Air with a Fuel-Rich, Reacting Crossflow, *Journal of Propulsion and Power*, **15**, 1999, 617-622.